Available online at www.sciencedirect.com
ScienceDirect
International Journal of Heat and Mass Transfer 51 (2008) 1480–1487
International Journal of HEAT and MASS TRANSFER
www.elsevier.com/locate/ijhmt

Technical Note

# Pyrolysis of a finite thickness composite material

M.A. Delichatsios *, J. Zhang

*FireSERT, School of Build Environment, University of Ulster at Jordanstown, BT37 0QB, UK*

Received 17 January 2007
Available online 4 January 2008

**Abstract**

A novel and complete methodology is presented to deduce a newly discovered (third type) steady state pyrolysis (ablation) rate on a composite material consisting of a pyrolysing material with inert backing when the composite material is exposed to a constant heat flux. The other two commonly known steady pyrolysis rates manifest when the pyrolysing material is thermally thick and when the temperature throughout the pyrolysing material is equal to its pyrolysis temperature. The value of the third type steady pyrolysis rate is accurately determined in terms of the thermal and pyrolysis properties of the composite material together with a delineation of the conditions under which it can be attained. The results are significant both for designing heat shields and for investigating the pyrolysis properties of materials in cone calorimeter type apparatus.


*Keywords:* Ablation; Pyrolysis of thermoplastics; Composite materials

## 1. Introduction

In a recent paper [1] Lin discovered a new steady state ablation (pyrolysis) rate solution for an ablating (pyrolysing) material supported on an inert substrate material, where a constant heat flux is applied on the ablating material and both materials have finite thickness with the inert material insulated at its back surface. The new steady state supplements two other steady state solutions one when the pyrolysing material is thermally thick (regression velocity $V_2$) and the other when its temperature is uniform and equal to the pyrolysis temperature (regression velocity $V_1$) [2,3]. The new solution applies after a long unsteady period from the beginning of the pyrolysis process when the thickness of the pyrolysing material has been reduced. However, Lin [1] was not quite sure in his paper under what conditions the new solution applies. We present a new derivation of this steady state solution to show that this solution exists at late times assuming that (a) the regression velocity ($V_3$) at this stage is less than the maximum possible regression velocity ($V_1$) which would occur if the temperature of the pyrolysing material was equal to its pyrolysis temperature and (b) the ratio of the thermal inertia of the pyrolysing material over its value for the inert material is less than one (i.e. $k_1\rho_1c_1/k_2\rho_2c_2 < 1$). The latter restriction is much milder than the requirement in [1] that the thermal inertia ratio should be much less than one (i.e. $k_1\rho_1c_1/k_2\rho_2c_2 \ll 1$), and the steady state solution is different from the one reported in [1]. However, the new steady solution will be reached if the transient time (starting when interaction occurs with the inert layer) towards this solution is less than the time required for the materials to completely pyrolyse. The present derivation also illustrates the physics in a more transparent way than in Lin's paper [1].

In addition to the significance for ablation [1], the present results apply for thermoplastics materials that behave as assumed in the paper, especially for test methods in fire research that essentially reproduce the situation of this paper. The basic test method is the cone calorimeter where a sample 100 × 100 mm is exposed to a constant heat flux in a nitrogen or ambient air atmosphere [3]. The sample is

* Corresponding author. Tel.: +44 (0)2890 368754; fax: +44 (0)2890 368726.
*E-mail address:* m.delichatsios@ulster.ac.uk (M.A. Delichatsios).

0017-9310/$ - see front matter © 2007 Elsevier Ltd. All rights reserved.
doi:10.1016/j.ijheatmasstransfer.2007.10.016

contained in a holder and the sample's back surface is insulated or in contact with a conductive material [3].

## 2. Methodology

We consider the same geometry as in [1] but the terminology is sometimes the one more commonly used in fire science. The ablating (pyrolysing) layer (denoted by the subscript 1) lies on an inert material (denoted by the subscript 2) as shown in Fig. 1. A constant heat flux $\dot{q}''_{ex}$ is applied on the top of the ablating material. The back surface of the inert material is insulated. The thermal properties of the ablating and inert material are denoted as $k_1, \rho_1, c_1$ and $k_2, \rho_2, c_2$, respectively. The latent heat of ablation pyrolysis is denoted as L. Perfect contact between the two-layers is assumed because the system represents a composite material.

We analyze first the inert layer considering a time dependent heat flux applied on it. This heat flux may for example represent the heat flux at the interface between the pyrolysing and the inert region. We show using a novel derivation that at late times greater than the diffusion penetration time $\ell_2^2/\alpha_2$, the imposed transient heat flux is proportional to the rate of change of temperature at its top surface multiplied by the heat capacity of the inert layer. This proportionality constant is equal to one for time varying polynomial heat fluxes but different from one for time varying exponential heat fluxes which are relevant to the present situation. Then, we use this condition for the back surface of the pyrolysing layer to find the new steady state regression solution for the pyrolysing layer.

### 2.1. The inert layer

A time varying heat flux $\dot{q}''_2(t)$ is applied on the front surface as shown in Fig. 2. The initial temperature is constant throughout the layer.

The normalized heat transfer equations are:

$$\frac{\partial\theta}{\partial t} = \frac{\partial^2\theta}{\partial x^2} \quad \text{where} \quad t = \frac{\alpha_2\tau}{\ell_2^2} \quad \text{and} \quad x = \frac{\eta}{\ell_2} \tag{1a}$$

where $\theta = (T(x,t) - T_0)/T_0$ with $T_0$ being the initial reference temperature, $\tau$ is the dimensional time, and $\eta$ is the distance from the top surface of the inert layer.

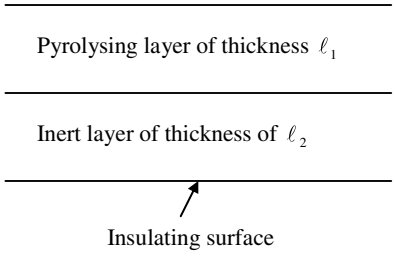


Fig. 1. A composite material consisting of an ablating (pyrolysing) layer and an inert insulated substrate.

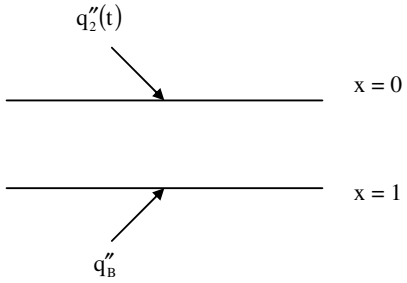


Fig. 2. Single inert layer heat transfer situation.

The boundary conditions are:

$$-\left.\frac{\partial\theta}{\partial x}\right|_{x=0} = \frac{\dot{q}''_2\ell_2}{k_2T_0} = q''_{2,F} \quad \text{and} \quad -\left.\frac{\partial\theta}{\partial x}\right|_{x=1} = q''_B \tag{1b}$$

To solve Eq. (1) we use first a special Laplace transform in space,

$$\widehat{\theta}(s,t) = \int_0^1 e^{-sx}\theta(x,t)\,dx \tag{2}$$

so that Eq. (1a) becomes:

$$\frac{\partial\,\widehat{\theta}}{\partial t} = s^2\,\widehat{\theta} + \left\{\left(-q''_B + s\theta_{x=1}\right)e^{-s} - \left(-q''_{2,F} + s\theta_{x=0}\right)\right\} \tag{3}$$

This equation can be formally solved in the time domain as:

$$\widehat{\theta}(s,t) = e^{s^2t}\int_0^t e^{-s^2\tau}G(s,\tau)\,dx \tag{4a}$$

where the function $G$ represents the term in big parenthesis in Eq. (3):

$$G = \left\{\left(-q''_B + s\theta_{x=1}\right)e^{-s} - \left(-q''_{2,F} + s\theta_{x=0}\right)\right\} \tag{4b}$$

By using now the Laplace transform in time:

$$\Theta = \int_0^\infty e^{-\varphi t}\,\widehat{\theta}(s,t)\,dt \tag{4c}$$

Eq. (4) becomes:

$$\Theta = \frac{\int_0^\infty e^{-\varphi t}G(s,t)\,dt}{\varphi - s^2} \tag{5}$$

Because this equation has to be finite for $s = \pm\sqrt{\varphi}$ the numerator must be equal to zero for these values. Thus, we obtain:

$$\int_0^\infty e^{-\varphi t}\left\{\left(-q''_B + \theta_{x=1}\sqrt{\phi}\right)e^{-\sqrt{\varphi}} - \left(-q''_{2,F} + \theta_{x=0}\sqrt{\phi}\right)\right\}dt = 0 \tag{6a}$$

and

$$\int_0^\infty e^{-\varphi t}\left\{\left(-q''_B - \theta_{x=1}\sqrt{\phi}\right)e^{-\sqrt{\varphi}} - \left(-q''_{2,F} + \theta_{x=0}\sqrt{\phi}\right)\right\}dt = 0 \tag{6b}$$

or in terms of Laplace transform in time (i.e. Eq. (4c)) these relations become:

$$-Q''_{\mathrm{B}}e^{-\sqrt{\varphi}}+\Theta_{x=1}\sqrt{\phi}e^{-\sqrt{\phi}}+Q''_{2,F}-\Theta_{x=0}\sqrt{\phi}=0 \tag{7a}$$

and

$$-Q''_{\mathrm{B}}e^{\sqrt{\phi}}-\Theta_{x=1}\sqrt{\phi}e^{\sqrt{\phi}}+Q''_{2,F}+\Theta_{x=0}\sqrt{\phi}=0 \tag{7b}$$

Here the capital letters represent the Laplace transform in time (Eq. (4c)) of the underlying quantities which are only function of time. Eqs. (7a) and (7b) are general expressions and provide the surface and interface temperatures and hear fluxes if two of these quantities are given. For the present case in Fig. 2, the back surface is insulated (i.e. $Q''_{\mathrm{B}}\equiv 0$) and elimination of the temperature $\Theta_{x=1}$ from Eqs. (7a) and (7b) gives the transformed heat flux as a function of the transformed heat flux at the surface:

$$Q''_{2,F}=\Theta_{x=0}\sqrt{\phi}\frac{e^{\sqrt{\phi}}-e^{-\sqrt{\phi}}}{e^{\sqrt{\phi}}+e^{\sqrt{\phi}}} \tag{7c}$$

It is possible to find the long time ($t=\alpha_2\tau/\ell_2^2\gg 1$) behaviour of the underlying quantities of the time Laplace transform in Eq. (7c) by noting that this behaviour in the Laplace domain corresponds to small values of Laplace variable $\phi$. Using simple expansion and keeping only the first order term, Eq. (7c) gives the following relation:

$$Q''_{2,F}=\phi\Theta_{x=0} \tag{8a}$$

In the time domain, this gives the relation for large times between the heat flux and the temperature at the front surface:

$$q''_{2,F}(t)=\frac{d\theta_{x=0}}{dt}\quad\text{for } t\to\infty \tag{8b}$$

or in terms of dimensional quantities (see Eqs. (1a) and (1b))

$$q''_2(t)=\rho_2c_2\ell_2\frac{d(T(x,t))_{x=0}}{d\tau}\quad\text{for } t\to\infty \tag{8c}$$

or more precisely,

$$\rho_2c_2\ell_2\frac{d(T(x,t))_{x=0}}{d\tau}\Big/q''_2(t)\to 1\ \text{for } t\to\infty \tag{8d}$$

Further examination showed that Eq. (8d) is correct only if the time variation of heat flux is a power law but it needs modification if the time variation of heat flux is exponential, which is a relevant case for the present problem. If the dimensionless heat flux varies as $e^{t/t_1}$, its time Laplace transform is $1/(\phi-1/t_1)$ and from Eq. (7c) the Laplace transform of temperatures at large times (i.e. small $\phi$) is:

$$\Theta_{\eta=0}=\frac{1}{\phi-1/t_1}\left(1+\frac{1}{3}\phi-\frac{1}{45}\phi^2+\ldots\right) \tag{9a}$$

where we have retained second terms in the expansion for small $\phi$.

If we invert Eq. (9a) by setting $\phi=1/t_1$ in the parenthesis of Eq. (9a) and taking the time derivative we find that:

$$\frac{d\theta_{x=0}}{dt}\Big/q''_{2,F}(t)\to 1+\frac{1}{3}\frac{1}{t_1}-\frac{1}{45}\left(\frac{1}{t_1}\right)^2+\ldots \tag{9b}$$

$$\text{where } q''_{2,F}(t)=e^{t/t_1} \tag{9c}$$

or in terms of dimensional quantities:

$$\mathrm{RATIO}=\rho_2c_2\ell_2\frac{d(T(x,\tau))_{x=0}}{d\tau}\Big/q''_2(\tau)\to 1+\frac{1}{3}\frac{1}{t_1}-\frac{1}{45}\left(\frac{1}{t_1}\right)^2+\ldots \tag{9d}$$

and

$$t_1=\alpha_2\tau_1/\ell_2^2 \tag{9e}$$

This is a crucial result of this paper. Namely, we conclude that the long term behaviour of the ratio at the left hand side (LHS) of Eq. (9d) is a constant which is function of the growth factor $(1/t_1)$ in the exponential variation of the heat flux but not equal to one. The results of Eqs. (9d) and (9e) were also verified numerically as Figs. 3–5 illustrate.

Fig. 3 shows the variation with time of the sensible heat to the imposed heat flux $\left(\rho_2c_2\ell_2\frac{d(T(x,\tau))_{x=0}}{d\tau}\Big/q''_2(\tau)\right)$ when an exponential heat flux is applied on the surface of the inert material. This ratio takes on for large times a constant value which depends on the growth factor $1/t_1$ in consistency with the analytical solution for large times, i.e. Eq. (9d). It is noted for future exploitation that the transient time to reach the asymptotic solution increases as the growth factor decreases to a value about $t=\alpha_2\tau/\ell_2^2=0.3$. The asymptotic steady values of the ratio $\rho_2c_2\ell_2\frac{d(T(x,\tau))_{x=0}}{d\tau}\Big/q''_2(\tau)$ are plotted as a function of the growth factor $1/t_1$ in Figs. 4 and 5 for two different ranges of the growth factor, i.e. 0 to 10 and 0 to 1, respectively. The results in Fig. 5 verify the analytical Eq. (9d) for small

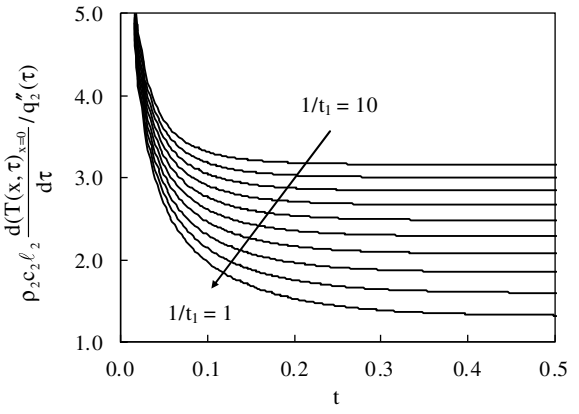


Fig. 3. Variation with time of the ratio $\rho_2c_2\ell_2\frac{d(T(x,\tau))_{x=0}}{d\tau}\Big/q''_2(\tau)$ when the heat flux is exponential with time $q''_2=e^{\tau/\tau_1}=e^{t/t_1}$ where $t=\alpha_2\tau/\ell_2^2$. At large times the ratio takes a constant value, which depends on the growth rate $1/t_1$.

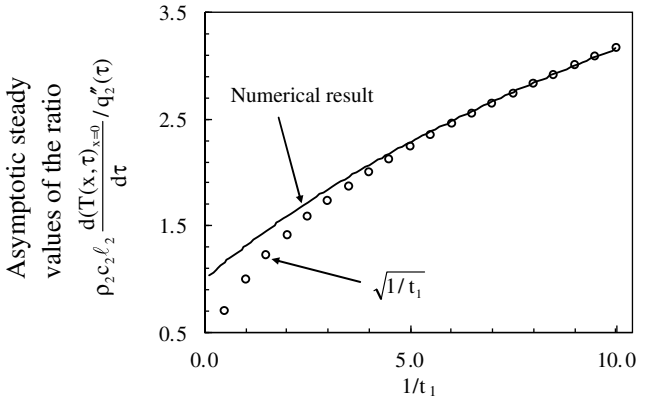


Fig. 4. The asymptotic steady ratio $G(\frac{1}{t_1}) = \rho_2 c_2 \ell_2 \frac{d(T(x,\tau))_{x=0}}{d\tau} \Big/ q_2''(\tau)$ as function of the growth parameter $1/t_1$ in the range of 0–10. The function $\sqrt{1/t_1}$ tends to the function $G(1/t_1)$ asymptotically for large values of $1/t_1$.

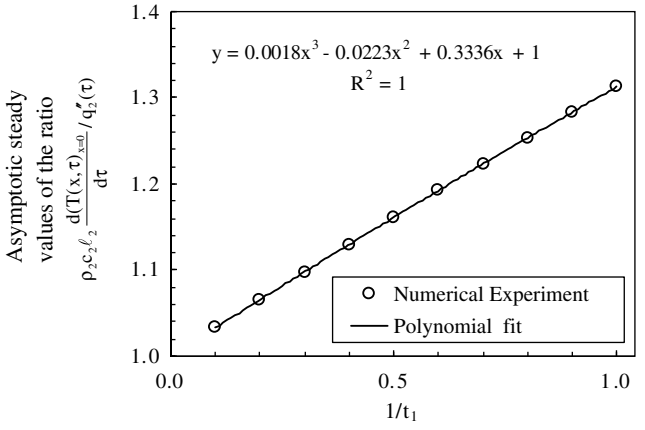


Fig. 5. The asymptotic steady ratio $\rho_2 c_2 \ell_2 \frac{d(T(x,\tau))_{x=0}}{d\tau} \Big/ q_2''(\tau)$ as function of the growth parameter $1/t_1$ in the range of 0–1.

values of $1/t_1$, whereas the results in Fig. 4 show that the ratio $\rho_2 c_2 \ell_2 \frac{d(T(x,\tau))_{x=0}}{d\tau} / q_2''(\tau)$ varies as the square root of the growth factor $(\sqrt{1/t_1})$ for large values of $1/t_1$. In summary:

$$\rho_2 c_2 \ell_2 \frac{d(T(x,\tau))_{x=0}}{d\tau} \Big/ q_2''(\tau) \to G(1/t_1) \tag{10a}$$

where

$$G(1/t_1) = 1 + \frac{1}{3}\frac{1}{t_1} - \frac{1}{45}\left(\frac{1}{t_1}\right)^2 + \ldots \text{ for } 1/t_1 \ll 1 \tag{10b}$$

$$G(1/t_1) = \sqrt{1/t_1} \text{ for } 1/t_1 \gg 1 \tag{10c}$$

The result of Eq. (10c) can also be derived directly from Eq. (7c) by noting that $\phi > 1/t_1 \gg 1$ so that $Q''_{2,F} = \Theta_{x=0}\sqrt{\phi}$, and hence following the same procedure in deriving Eq. (9b) from Eq. (9a).

This long time behaviour of the ratio $\rho_2 c_2 \ell_2 \frac{d(T(x,\tau))_{x=0}}{d\tau} \Big/ q_2''(\tau)$, as shown by Eq. (10a) and Figs. 4 and 5, is employed in the next sections as the boundary condition at the interface (see Fig. 1) to resolve the behaviour of the ablating (pyrolysing) layer at late times following its exposure to a constant heat flux.

### 2.2. The ablating/pyrolysing layer at late times

The ablating/pyrolysing layer is examined in dimensional coordinates as shown in Fig. 6 just before regression starts but assuming that the back boundary condition is determined by Eqs. (10a) and (10b) and the results in Figs. 4 and 5.

The heat transfer equation and the boundary conditions are:

$$\frac{\partial T}{\partial \tau} = \alpha_1 \frac{\partial^2 T}{\partial \eta^2} \tag{11a}$$

A steady regression solution with a rate $V_3$ is examined for its existence.

The boundary condition at the receding surface is:

$$-k_1 \frac{\partial T}{\partial \eta} = \dot{q}''_{\text{ext}} - \rho_1 L V_3 \text{ at } \eta = \text{front} = V_3 \tau \tag{11b}$$

and

$$T = T_p = \text{pyrolysis temperature at } \eta = \text{front} = V_3 \tau \tag{11c}$$

Here $\ell_1$ is the original thickness of the layer when the present steady solution applies. If a steady state regression ($V_3$) solution exists it must have the following form [1–3]:

$$T_p - T = C_0(1 - e^{-\{\eta - V_3\tau\}/\delta}) \tag{11d}$$

$$\text{where the thermal depth is } \delta = \alpha_1 / V_3 \tag{11e}$$

Eq. (11d) satisfies the boundary condition (11c) and the constant, $C_0$, is determined from the boundary condition (11b) as:

$$\frac{C_0}{\delta} = \dot{q}''_{\text{ext}} - \rho_1 L V_3 \tag{11f}$$

The solution Eq. (11d) is realistic if the temperature is less than the pyrolysis temperature everywhere and if the temperature at the interface is greater than the initial temperature $T_0$. The first condition requires $C_0$ being positive and the second condition requires the original thickness being

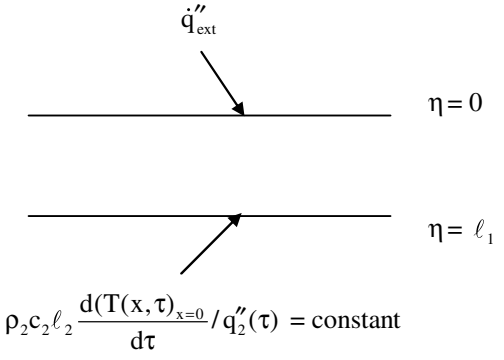


Fig. 6. The (top) ablating/pyrolysing layer.

less than a certain value. Mathematically these conditions are represented by:

$$\dot{q}''_{\text{ext}} - \rho_1 L V_3 > 0 \text{ or } V_3 < \frac{\dot{q}''_{\text{ext}}}{\rho_1 L} = V_1 \tag{12a}$$

$$T_{\text{p}} - T_0 < C_0(1 - \text{e}^{-\ell_1/\delta}) \tag{12b}$$

To combine this solution with the heat transfer into the inert sub-layer, we highlight from the solution Eq. (11d) the following boundary condition at the back surface of the pyrolysing layer, i.e. the interface with the inert layer:

$$-\frac{\partial T_{\text{int}}(\eta,\tau)}{\partial \eta} = \frac{q''_2(\tau)}{k_1} = \frac{1}{V_3}\frac{\partial T_{\text{int}}(\eta,\tau)}{\partial \tau} \text{ at } \eta = \ell_1 \text{ (and at } x = 0 \text{ of the inert layer)} \tag{12c}$$

We note by using (11d) and (12c) that the heat flux at the interface $q''_2(\tau)$ is an exponential function of time with a growth rate $\tau_1 = \frac{\delta}{V_3} = \frac{\alpha_1}{V_3^2}$, i.e. $q''_2(\tau) \propto \text{e}^{\tau\alpha_1/V_3^2}$. Applying the results of the previous section by inserting Eq. (12c) into Eq. (10a) we obtain:

$$\rho_2 c_2 \ell_2 \frac{\text{d}(T(x,\tau))_{x=0}}{\text{d}\tau} \Big/ q''_2(\tau) = \frac{V_3}{k_1/\rho_2 c_2 \ell_2} \to G(1/t_1) \tag{13a}$$

where the dimensionless growth factor $t_1$ (using the scaling for the inert layer) is:

$$t_1 = \frac{\alpha_2 \tau_1}{\ell_2^2} = \frac{\alpha_2 \alpha_1}{\ell_2^2 V_3^2} \tag{13b}$$

By defining a reference velocity as:

$$V_r = k_1/\rho_2 c_2 \ell_2 \tag{13c}$$

Eqs. (13a) and (13b) take the forms:

$$\frac{V_3}{k_1/\rho_2 c_2 \ell_2} = \frac{V_3}{V_r} = G(1/t_1) \tag{14a}$$

$$\text{where } t_1 = \frac{\alpha_2 \tau_1}{\ell_2^2} = \frac{\alpha_2 \alpha_1}{\ell_2^2 V_3^2} = \left(\frac{V_r}{V_3}\right)^2 \frac{k_2 \rho_2 c_2}{k_1 \rho_1 c_1} \tag{14b}$$

The function $G$ in Eq. (14a) is given asymptotically by Eqs. (10b) and (10c) and the complete numerical results are plotted in Figs. 4 and 5.

### 2.3. Determination of the new regression velocity

Eq. (14a), together with the definition of the function $G$ from Eqs. (10b) and (10c), determines the ratio $V_3/V_{\text{r}} = X$ from which the new regression velocity is found using the definition of the reference velocity in Eq. (13c). Specifically, Eq. (14a) is written as:

$$\frac{V_3}{k_1/\rho_2 c_2 \ell_2} = \frac{V_3}{V_r} = X = G(1/t_1) = G\left(X^2 \frac{k_1 \rho_1 c_1}{k_2 \rho_2 c_2}\right) \tag{15a}$$

From the approximate behaviour of the function $G$ for small and large values of its argument (i.e. Eqs. (10b) and (10c)), it can be seen that there is a solution of Eq. (15a) only if the ratio of the thermal inertia parameter is less than one, i.e.:

$$\frac{k_1 \rho_1 c_1}{k_2 \rho_2 c_2} = \text{TIP} < 1 \tag{15b}$$

In general Eq. (15a) implies that the steady regression velocity $V_3$ is a function of the TIP, namely:

$$\frac{V_3}{k_1/\rho_2 c_2 \ell_2} = \frac{V_3}{V_r} = X = \text{function of}\left(\frac{k_1 \rho_1 c_1}{k_2 \rho_2 c_2}\right) \tag{15c}$$

For small values of the argument of $G$, Eq. (15a) becomes following Eq. (10b):

$$X = G\left(X^2 \frac{k_1 \rho_1 c_1}{k_2 \rho_2 c_2}\right) = 1 + \frac{1}{3} X^2 \frac{k_1 \rho_1 c_1}{k_2 \rho_2 c_2} = 1 + \frac{1}{3} X^2 \text{TIP} \tag{15d}$$

whose solution representing the solution of Eq. (15a) for small values is:

$$X = \frac{V_3}{V_r} = \frac{1 - \sqrt{1 - 4(\text{TIP})/3}}{2(\text{TIP})/3} \tag{15e}$$

This approximate solution is a good approximation up to TIP = 0.5, after which its accuracy compared to the exact solution decreases. The exact solution of Eq. (15a) using the numerical form of the function $G$ is given in Appendix A.

The analytical solution results for the ratio $V_3/V_{\text{r}}$ are consistent with the results in [1] and verified by Figs. 7–9. Figs. 7 and 8 show the history of regression velocity for several sets of parameters normalized by using the properties of layer 2 as in [1] and defined here as:

$$H = \frac{\rho_1 L}{\dot{q}''_{\text{ext}}}\frac{\alpha_2}{\ell_2}, \quad U = \frac{T - T_{\text{p}}}{\ell_2 \dot{q}''_{\text{ext}}/k_1}, \quad A = \frac{\alpha_1}{\alpha_2}, \quad K = \frac{k_1}{k_2} \quad \text{and} \quad S = \frac{\ell_1}{\ell_2} \tag{16a}$$

The normalized regression velocity and time which are the coordinates in Figs. 7 and 8 are defined as:

$$\tilde{V} = \frac{V \ell_2}{\alpha_2} \text{ and } t = \frac{\alpha_2 \tau}{\ell_2^2} \tag{16b}$$

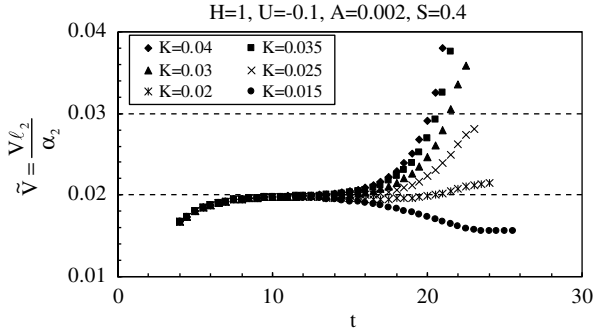


Fig. 7. Dimensionless regression history for $H = 1$ and the other properties stated in the legend. Eq. (1a) defines all the parameters in the legend.

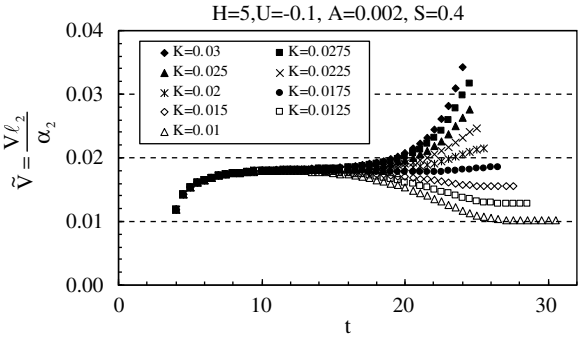


Fig. 8. Dimensionless regression history for $H = 5$ and the other properties in Fig. 7. Eq. (1a) defines all the parameters in the legend.

Figs. 7 and 8 present the numerical regression velocity as a function of time for the same properties of the composite layer except the latent heat flux being $H = 1$ for Fig. 7 and $H = 5$ for Fig. 8. In both situations after pyrolysis starts, a steady regression velocity $V_2$ exists corresponding to thermally thick conditions before the pyrolysing layer interacts with the inert layer:

$$\tilde{V}_2 = \frac{V_2 \ell_2}{\alpha_2} = \frac{\ell_2}{\alpha_2} \frac{\dot{q}''_{\text{ext}}}{\rho_1 (L + c_1 (T_p - T_0))} = \frac{1}{H - U_0/A} \tag{17}$$

where we have applied the definitions of Eq. (16).

At some point in Figs. 7 and 8 when the thermal depth $\alpha_1/V_2$ is equal to the thickness of the pyrolysing layer, the influence of the inert layer emerges and the regression velocity diverges from the value $V_2$. The new steady state pyrolysis develops in several cases whereas in the rest of the cases the pyrolysing material is consumed before the steady state is attained.

The steady state regression solutions are plotted in Fig. 9 in terms of the normalized velocity $V_3/V_r$ against the inverse thermal inertia parameter, 1/TIP. Not only there is good correlation of the data but even the approximate analytical solution, Eq. (15e), agrees very well with the numerical results.

In conclusion, we have shown that (a) the regression velocity at the late stages can exist for values of TIP $< 1$ and not only for TIP $\ll 1$ as [1] suggests and (b) its value can be greater than the reference velocity $V > V_r = k_1/\rho_2 c_2 \ell_2$ in contrast to [1] where $V = V_r$ is suggested. In the next section, we propose the conditions under which this late stage velocity has time to be reached before the pyrolysing material is consumed.

### 2.4. Existence of the late stage steady pyrolysis rate

This section discusses the conditions under which a steady pyrolysis rate might occur late in the pyrolysis process and the conditions this state can be actually reached during the heating and pyrolysis of a composite material as depicted in Fig. 1.

The first set of conditions have been obtained in the analysis up to this point and summarized as:

1. The thermal inertia parameter TIP must be less than one (see discussion related to Eqs. (15a) and (15b)):

$$\frac{k_1 \rho_1 c_1}{k_2 \rho_2 c_2} = \text{TIP} < 1 \tag{18a}$$

2. The late steady velocity and initial thickness of the pyrolysing region, when this velocity applies, should satisfy the following relations (see discussion related to Eqs. (12a) and (12b)):

$$V_3 < \frac{\dot{q}''_{\text{ext}}}{\rho_1 L} = V_1 \tag{18b}$$

$$T_p - T_0 < \frac{\alpha_1}{V_3} \left( \dot{q}''_{\text{ext}} - \rho_1 L V_3 \right) \left( 1 - e^{-\ell_1/\delta} \right) \tag{18c}$$

If the conditions delineated by Eqs. (18a), (18b), and (18c) are satisfied, then the steady state velocity $V_3$ is defined by Eqs. (15a)–(15d). But even if these conditions

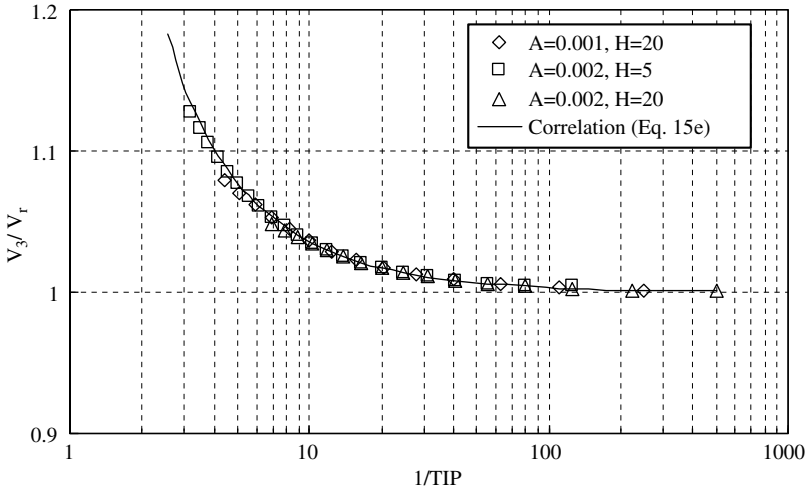


Fig. 9. Steady state regression velocity against the inverse TIP. Eq. (1a) defines all the parameters in the legend.

are met, the steady state pyrolysis at late stages may not be reached because there are not sufficient times for these conditions to establish.

The significant times for the pyrolysis process of the composite material are:

1. The time for the inert layer to reach the state for which the ratio $\rho_2 c_2 \ell_2 \frac{d(T(x,\tau))_{x=0}}{d\tau} \Big/ q''_2(\tau)$ (see Fig. 2) is constant. This time is of the order of the diffusion time in the inert layer:

$$\tau_1 = \frac{\ell_2^2}{\alpha_2} \tag{19a}$$

2. The time for the steady state velocity to change from $V_2$ (the regression velocity for thermally thick conditions) to $V_3$ the new late stage steady solution. Here, we consider only the cases that a steady state regression solution develops corresponding to thermally thick conditions before interaction with the inert layer leads to the new regression velocity. The interaction with the inert layer occurs when the thickness of the pyrolysing layer is equal to the thermal thickness of the pyrolysing layer:

$$\delta = \frac{\alpha_1}{V_2} \tag{19b}$$

and the time of transition would be of the order:

$$\tau_2 = \delta / V_2 = \frac{\alpha_1}{V_2^2} \tag{19c}$$

This result can also be found from a rather simplified energy integral balance in the pyrolysing layer.

3. The time for the pyrolysing material to be completely consumed. This time consists of the time needed for the pyrolysing material to pyrolyse plus the time needed for the inert layer to be heated to the conditions corresponding at the end of the pyrolysing process. Namely, this time will be:

$$\tau_{\text{total}} = \frac{\ell_1}{V_2} + \frac{Q''}{\dot{q}''_{\text{ext}}} \tag{19d}$$

where the heat accumulated per unit surface area in the inert material at the end of pyrolysis is given by:

$$Q'' = \rho_2 c_2 \ell_2 (T_p - T_0) - \frac{1}{3}\left(\dot{q}''_{\text{ext}} - \rho_1 L V_3\right) \tag{19e}$$

This relation was derived in a similar way as in [1] by approximating the profile of temperature in the inert material as a parabolic profile which is appropriate for values of TIP $\ll 1$. For comparison with the other times, we should evaluate the complete pyrolysis time after interaction of the pyrolysing layer with the inert layer starts namely when the thickness of the pyrolysing layer is $\delta = \ell_1 = \alpha_1 / V_2$. It follows that the relevant time for complete consumption of the pyrolysing layer will be:

$$\tau_3 = \frac{\alpha_1}{V_2^2} + \frac{\rho_2 c_2 \ell_2 (T_p - T_0) - \frac{1}{3}\left(\dot{q}''_{\text{ext}} - \rho_1 L V_3\right)}{\dot{q}''_{\text{ext}}} \tag{19f}$$

or

$$\tau_3 = \frac{\alpha_1}{V_2^2} + \frac{\rho_2 c_2 \ell_2 (T_p - T_0)}{\dot{q}''_{\text{ext}}} - \frac{1}{3}(1 - V_3/V_1) \tag{19g}$$

The late stage solution will be attained if there is sufficient time for the inert layer to reach its asymptotic behaviour and the transition time to the late stage regression rate is less than the consumption time of the pyrolysing material. This statement is expressed by the requirement that:

$$\tau_1 < \tau_2 < \tau_3 \tag{20}$$

Examination of the numerical data in [1] and numerical data in this work support the applicability of Eq. (20) as an order of magnitude relation. The first part of the inequality in Eq. (20) is the most critical for a steady late stage solution to be attained or to be developing but not reached because the pyrolysing material is consumed.

## 3. Conclusions

The major contributions of this work are:

- The new steady state solution discovered by Lin [1] has a much greater range of applicability being possible for the thermal inertia parameter $\frac{k_1 \rho_1 c_1}{k_2 \rho_2 c_2} = \text{TIP} < 1$ and not $\ll 1$ as proposed by Lin [1].
- The regression velocity at the new steady state conditions, is a function of the TIP and higher than the velocity proposed in [1].
- The new steady state solution is attainable if there is sufficient time for the inert layer to reach its asymptotic behaviour and the transition time to the late stage regression rate is less than the consumption time of the pyrolysing material, as expressed by Eq. (20).
- In developing the present analysis a new method was applied to obtain the long term heating behaviour of the inert layer culminating to the relation given by Eq. (7c), and the asymptotic result at the interface given by Eqs. (10a)–(10c).

We must reiterate here hat in addition to the significance for ablation [1], the present results apply for thermoplastics materials that behave as assumed in the paper, especially for test methods in fire research that essentially reproduce the situation of this paper. The basic test method is the cone calorimeter where a sample 100 × 100 mm is exposed to a constant heat flux in a nitrogen or ambient air atmosphere [3]. The sample is contained in a holder and the

sample's back surface is insulated or in contact with a conductive material [3].

## Appendix A. Complete solution of Eq. (15a) for $V_3/V_r$

Eq. (15a) is written as:

$$\frac{V_3}{V_r} = G\left[\left(\frac{V_3}{V_r}\right)^2 \frac{k_1\rho_1 c_1}{k_2\rho_2 c_2}\right] \tag{A1}$$

or by using the relation $\frac{1}{t_1} = G\left(\frac{V_3}{V_r}\right)^2 \frac{k_1\rho_1 c_1}{k_2\rho_2 c_2}$, we have:

$$\frac{V_3}{V_r} = \sqrt{\frac{1/t_1}{TIP}} = G\left(\frac{1}{t_1}\right) \tag{A2}$$

The right hand side (RHS) of Eq. (A2) is determined for the total range of $1/t_1(0 \to \infty)$ numerically (see Figs. 4 and 5), and is plotted in Fig. A1. Superimposed on this, the LHS of Eq. (A2) is plotted for various values of TIP from 0 to 1 in Fig. A1. The interception of these curves gives the solution of Eq. (A2), which is plotted in Fig. A2.

The late stage velocity is found for $\frac{V_3}{V_r} = \sqrt{\frac{1/t_1}{\mathrm{TIP}}}$, and is plotted in Fig. A3, together with the approximate solution given by Eq. (15e). The agreement between these two solutions, i.e. the "exact" and the approximate, is very good up to a value of TIP = 0.5.

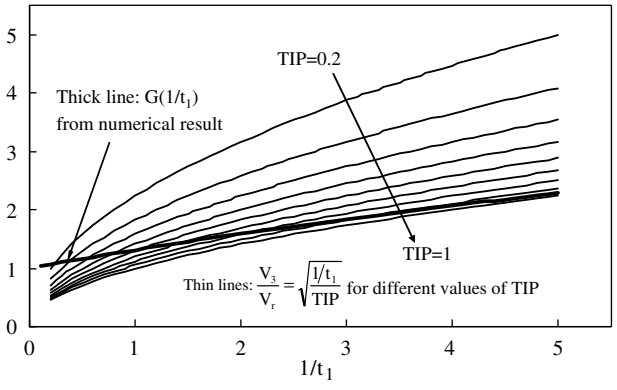


Fig. A1. Numerical result of $G(1/t_1)$ and a geometrical view of the dimensionless velocity $V_3/V_r = \sqrt{1/t_1/\mathrm{TIP}}$ with TIP from 0.2 to 1.0, representing the solution of Eq. (A1).

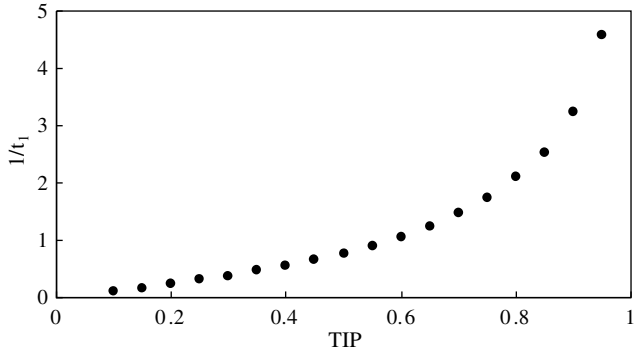


Fig. A2. Values of $1/t_1$ corresponding to the intercepts of the numerical result and $\sqrt{1/t_1/\mathrm{TIP}}$ with TIP from 0.1 to 0.95 (see Eqs. (A1) and (A2)).

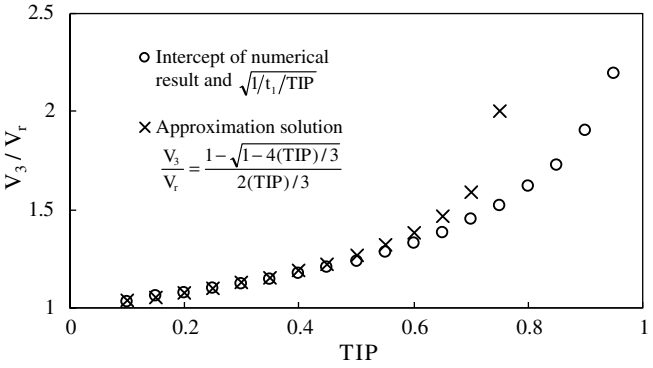


Fig. A3. Dimensionless velocity $V_3/V_r$ derived from the intercepts of the numerical result and $\sqrt{1/t_1/\mathrm{TIP}}$ with TIP from 0.1 to 0.95, and from the analytical solution (see Eqs. (A1) and (A2)).

## References

[1] F.S. Lin, Steady ablation on the surface of a two-layer composite, Int. J. Heat Mass Transfer 48 (2005) 5504–5519.
[2] Y. Chen, M.A. Delichatsios, V. Motevalli, Material Pyrolysis Properties Part I, Combust. Sci. Technol. 88 (1993) 309–328.
[3] J. Zhang, J. Hereid, M. Hagen, D. Bakirtzis, M.A. Delichatsios, Numerical and experimental investigation of ignition and pyrolysis of Polyamide nylon nanocomposites, 11th European Meeting on Fire Retardant Polymers, Bolton, 2007 (also submitted for publication in Fire and Materials).